ARTICLE IN PRESS

Journal of King Saud University – Computer and Information Sciences xxx (xxxx) xxx

Contents lists available at ScienceDirect

Journal of King Saud University – Computer and Information Sciences

journal homepage: www.sciencedirect.com

# Moving objects multi-classification based on information fusion

Bouchra Honnit [a,*], Khaoula Belhaj Soulami [a], Mohamed Nabil Saidi [b], Ahmed Tamtaoui [a]

[a] Multimedia, Signal and Communication System (MUSICS), National Institute of Posts and Telecommunication (INPT), Postal code: 10112, Rabat, Morocco
[b] SI2M Laboratry, National Institute of Statistics and Applied Economy (INSEA), Postal code: 10112, Rabat, Morocco

ARTICLE INFO

*Article history:*
Received 3 September 2019
Revised 27 February 2020
Accepted 7 May 2020
Available online xxxx

*Keyword:*
Moving objects classification
Multi-classification
Video surveillance system
Score level fusion
Late fusion
T-conorm operator

ABSTRACT

This paper aims to present a new model for multi-classification in video surveillance, based on data fusion. First, features are extracted. Then, a pre-classification is conducted using each feature separately. Second, the obtained posterior probabilities, are combined using the T-conorm operator. At last, the maximum is applied to specify the label of each detected object. The performance of our model was evaluated using two public datasets. In addition, the used number of classes and features were varied, in order to, validate the efficiency of our model. The obtained results showed that our model improved the classification accuracy up to an average of 99% using SVM, also, it outperformed the other methods.


## 1. Introduction

Moving object classification plays a important role in many computer vision applications such as event understanding (Chapman et al., 2019; Cheng et al., 2019; Xu et al., 2019), human action recognition (Zhang and Tao, 2019; Avola et al., 2019; Liu et al., 2019), vehicles tracking (Zhao et al., 2019; Kwan et al., 2019; Cui et al., 2019), and smart video surveillance systems (Karthikeswaran et al., 2019; Muchtar et al., 2019; Savvides et al., 2019). It aims to identify the category, called also label, of a detected object based on two main steps. First, one or several features are extracted using the bounding box, the contour, the texture, or the movement vector of the detected moving objects. Second, they are fed to a defined classifier in order to specify the class of each object. However, it is a challenging task, due to the real-world constraints and dynamic weather conditions (e.g. rainy day, high illumination, camera movement). Moreover, the classification process should be robust to the object scale, translation, and rotation variation.

To improve the classification accuracy, researchers have proposed several approaches, i.e. definition of new features, the combination of several features and classifiers, usage of binary classification instead of a multi-classification. However, for the case of video surveillance system, using only two classes is not suitable since several objects pass in front of the camera. In the other hand, combining several features results a high dimensional matrix which will increase significantly the computational time. Therefore, we propose in this study a new model for moving objects multi-classification based on late fusion using the T-conorm operator.

This paper is organized as follows: first in Section 2, we review the related works. In Section 3, we give a background theory. In Section 4, we describe the proposed model. Then in Section 5, we present the obtained results that will be discussed in Section 6. Finally, we give the conclusion.

## 2. Related works

In our knowledge, the current state of the art regarding the improvement of the classification accuracy of moving objects in surveillance videos can be grouped into two main categories, feature-based approaches and classifier-based techniques. We present these existing researches as follows:

The existing feature-based methods consist of applying new features or combining features or selecting relevant features. In the current literature the most used features in moving object classification can be categorized into Shape-based features, texture-

* Corresponding author.
*E-mail address:* honnit@inpt.ac.ma (B. Honnit).

Peer review under responsibility of King Saud University.

Production and hosting by Elsevier

https://doi.org/10.1016/j.jksuci.2020.05.003
1319-1578/

Please cite this article as: B. Honnit, K. B. Soulami, M. N. Saidi et al., Moving objects multi-classification based on information fusion, Journal of King Saud University –
Computer and Information Sciences, https://doi.org/10.1016/j.jksuci.2020.05.003

based features, and motion-based features. Jabri et al. (2018) proposed a real-time system for the detection and classification of vehicles. The authors used the canny edge detection method to extract the shape information from the detected vehicles, and then they classified them into car or bike. Patil and Nandyal (2013) used the canny edge detector to extract shape features from the detected vehicles in traffic surveillance videos. The extracted vehicles were then classified into two or four-wheel vehicles using a neural network model. Sehairi et al. (2018) proposed a system for the aging person falls. The authors also used shape features to extract the silhouette information of an elderly falling. The texture-based descriptors are also widely used for the detection and classification of moving objects. Al Jarouf and Kurdy (2018) proposed a system for vehicle crash detection. The authors extracted Haar-Like features from the detected vehicle crash, then used them to train a pre-train SVM classifier. Luo et al. (2019) used also Haar features and SVM classifier for car detection. The authors' method focused on optimizing the hardware tradeoff, which relies between minimizing the memory resources and maximizing the processing speed and recognition accuracy. The motion-based features are also widely used in the detection of moving objects. For instance, Saeed et al. (2019) used Low-rank Sparse Aggregate Channel Features (SACF) for person identification in surveillance videos. The authors then conducted the classification process based on an SVM classifier. Wang et al. (2019) used multiple spatio-temporal features for the vehicle detection in surveillance videos. The authors have improved the feature extraction algorithm, spatio-temporal sample consistency algorithm.

The previously mentioned methods focused on a specific problem, which requires the classification of one or two moving objects. In this case, the number of classes cannot exceed one or two, as one type of features will not hold enough information about the detected objects. To tackle this limitation, some of the researchers relied on combining multiple features to get a sufficient description and information of the detected objects. For instance, Bogomolov et al. (2003) used the combination of the shape and motion features for the detection of moving targets in natural and real-life settings. The authors tested the extracted features using the SVM classifier and shows how the combination of the two categories of the used features helps improving the classification accuracy rather than using them separately. Alamgir et al. (2018) proposed a new feature for the detection of smoke in surveillance videos. This feature is based on the combination of textural local binary co-occurrence descriptors and color-based RGB multi-channel features. The extracted features were then fed to a support vector machine (SVM) classifier. For a better recognition of actions, Ikizler-Cinbis and Sclaroff (2010) proposed an approach based on the combination of features extracted from the detected person, objects, and scenes. The action in videos was recognized by feeding the features into a Multiple Instance Learning (MIL) paradigm. Mahalingam and Subramoniam (2018) used texture-based and quality-based features. These features were merged and tested on a decision tree classifier. The classification results were compared with two other classifiers, K-nearest neighbor (KNN) and Multi-layer Perceptron (MLP).

The combination of features does not help all the time getting the best classification accuracy. In most of the cases, we get redundant and repetitive information from merging the features using a simple combination approaches. This can be expensive in terms of the classification's processing time. In response to these drawbacks, some techniques relied on feature selection methods to extract as many concise and informative features as possible. For instance, Laopracha et al. (2019) proposed a method for the selection of relevant patterns of histograms of oriented gradients (HOGs) in vehicle detection. In fact, the HOG method generates both redundant and ambiguous, which may bias the classification process. The authors tested the selected features using different classifiers including, a support vector machine, K-nearest neighbor, random forest, and deep neural network. Recently, metaheuristic algorithms have been used in many fields (Soulami et al., 2018; Soulami et al., 2019; Soulami et al., 2017; Soulami et al., 2016) including moving object detection (Vijayan and Ramasundaram, 2019; Lee et al., 2015) and particularly in the feature selection phase. For instance, Jemilda and Baulkani (2018) extracted multiple features for the classification of moving object including, a shape-based feature, Speeded Up Robust Features (SURF), a texture-based feature, Enhanced Local Vector Pattern (ELVP), and a color-based feature, Histogram of Gradient (HOG). The authors then used the metaheuristic technique, Genetic Algorithm (GA) for feature selection to reduce the dimensionality and to produce a relevant feature from the previously mentioned descriptors. Shi et al. (2018) combined the metaheuristic algorithms genetic algorithm (GA) and tabu search (TS) for feature selection in object detection. The authors address the premature convergence of the GA algorithm by using the TS algorithm. The features are then fed to an SVM classifier. Mohamed et al. (2019) proposed a novel metaheuristic algorithm for feature selection in moving objects detection. Their proposed approach called, Parasitism – Predation algorithm (PPA) helps solve the dimensionality curse, then the K nearest neighbor (KNN) classifier was used to evaluate the performance of the selected features.

In all the previously mentioned papers, we do not know which features contribute the most to the detection and recognition of a specific target or class. Nor do we know the reason behind selecting each feature. In fact, a feature can be relevant and helps detecting an object, but may fail in recognizing others, because it may hold information that describe that target better than the other ones. Hence, some researchers focused on combining and merging the classifier's decision instead of dealing with the feature selection optimization. For instance, Zhao et al. (2014) proposed a multi-classifier fusion for pedestrian detection. After extracting the Histogram of Oriented Gradient (HOG) feature to describe the pedestrian and non-pedestrians. The authors reduced the dimension of the extracted features using Principal Component Analysis (PCA) technique to decrease the processing time and keep the relevant features. The classification process was then performed based on the fusion of three classifiers including, Support Vector Machine (SVM), Naïve Bayesian, and Minimum Distance Classifier. Wei et al. (2019) extracted the Haar and HOG features to describe multi-vehicles characteristics. The authors then used a cascade structured AdaBoost classifier for the classification of the multi-vehicles and an SVM classifier for a further and precise target detection.

Recently and with the emergence of ground breaking artificial intelligence techniques. Deep learning models are getting more and more attention from the authors working on moving object detection and classification. For instance, Chen et al. (2019) proposed a novel distributed video surveillance system. The system is based on a deep learning model that reduces the huge network communication and solves the problems related to parallel training and model synchronization. Sun et al. (2019) proposed also an end-to-end deep learning classifier based on convolutional neural network and one-class Support Vector Machine (SVM) classifier. The proposed algorithm simplifies the complexity of the process and attain a global optimal solution. Moreover, the loss function used in the model derived was derived from a one-class Support Vector Machine (SVM) classifier is used in the optimization of the proposed model's parameters. Although, deep-learning approaches outperformed methods using the machine learning algorithms, unfortunately, some problems are encountered and resumed as follow:

Please cite this article as: B. Honnit, K. B. Soulami, M. N. Saidi et al., Moving objects multi-classification based on information fusion, Journal of King Saud University – Computer and Information Sciences, https://doi.org/10.1016/j.jksuci.2020.05.003

- Deep learning model is based on a specific image size. Researchers proposed the use of the re-sizing layer. However, they proved that by re-sizing the images, the information become useless and less informative;
- Workstation machine is needed to train a deep learning model; otherwise the execution time becomes very long;
- The larger the size of the data, the better a deep learning model is expected to perform. However, this huge amount of data does not exists in the fields of video surveillance system.

## 3. Background theory

### 3.1. Information fusion

Information fusion is the combination of data originating from several sources, in order to improve the decision-making. Usually, it is applied at four levels:

- Sensor level: combine the raw data from different sources;
- Feature level: combine the extracted features;
- Score level: combine the matching scores provided by different classifiers;
- Decision level: combine the obtained decisions by an individual classifier.

In our work, we focus on the score level fusion. It is achieved by conducting the classification using the same classifier for each feature separately. The fusion is based on T-conorm operator and compared with two fusion methods *(FMR)*: rules based on probability approach and majority vote rule.

**Rules based on the probability** This approach is based on combining the offered scores by the classifiers, which are the posterior probabilities $sr_k = s_{i,j}^k = P(\omega_k \mid x_{i,j}^k)$. Where $P(\omega_k \mid x_{i,j}^k)$ is the posterior probability of the class $w_k$ offered by the source $k$ using the feature $s_{i,j}$. There are three ways to combine these probabilities:

- Median rule (mean): $max_{k=1,\cdots,c} med_{j=1}^{M} P(\omega_k \mid x_{i,j}^k)$
- Sum rule: $max_{k=1,\cdots,c} \sigma j = 1^M P(\omega_k \mid x_{i,j}^k)$
- Min rule: $max_{k=1,\cdots,c} \min_{j=1}^{M} P(\omega_k \mid x_{i,j}^k)$

In our study we investigate the median rule.

**Majority vote rule** is the simplest fusion method. It consists on computing the number of time that each class appeared, and the winning class $w_{class}$ is the most appeared one.

$$w_{class} = argmax_{k=1,\cdots,c} \Sigma_{j=1}^{M} \alpha_j Q_{jk} \quad (1)$$

where:

$$Q_{jk} = \begin{cases} 1 & if \quad p(\omega_k \mid X_j) = \max_{i=1,\cdots,c} P(\omega_k \mid X_j) \\ 0 & otherwise \end{cases} \quad (2)$$

And

$$\Sigma_{j=1}^{M} \alpha_j = 1 \quad (3)$$

The coefficient $\alpha_j$ is the reliability degree of the classifier and it can be estimated by the recognition rate of each classifier. It is used to solve the conflict problem between the classifier. This coefficient is omitted, since, in our case we used only one classifier.

### 3.2. T-conorm operator

T-conorm operators belong to the Triangular operators, called also T-operators. They appeared for the first time in the statistical context (i.e. probabilistic metric space) Schweizer and Sklar

**Table 1**
T-conorm operators.

| | |
|---|---|
| Zadeh | $max(x, y)$ |
| Probabilistic (Prob) | $x + y - xy$ |
| Lukasiewicz (Luka) | $min(x + y, 1)$ |
| Einstein (Ein) | $\frac{x+y}{1+xy}$ |

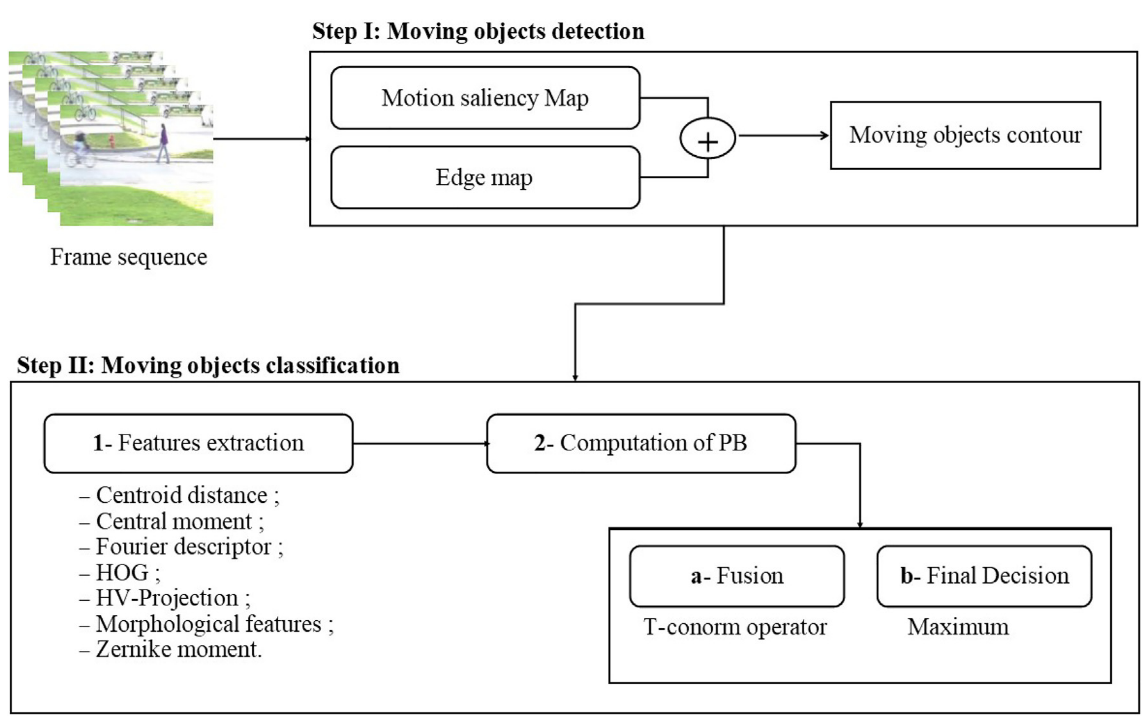


**Fig. 1.** Proposed model for moving object detection and classification.

Please cite this article as: B. Honnit, K. B. Soulami, M. N. Saidi et al., Moving objects multi-classification based on information fusion, Journal of King Saud University – Computer and Information Sciences, https://doi.org/10.1016/j.jksuci.2020.05.003

(1960); Schweizer, 1983. It has been observed that the choice of a suitable T-operator can considerably enhance the performance of the used system. T-conorm operators are used to compute the union of sets. Mathematically, it is a two-place function $T:[0,1]\times[0,1]\longrightarrow[0,1]$, defined by $S(x,y)=1-T(1-x,1-y)$ which is associative, commutative, with 0 as unit and non-decreasing in each place.

There exist several definitions for T-conorm operator. However, in our study we selected only the very known ones Table 1.

## 4. The proposed model

As Fig. 1 shows, our system starts with a moving object detection step and finishes with a classification process. In the first step, each moving object is extracted. Then, its corresponding label is specified in the second step.

In fact, the detection process is based on our previously published work Honnit et al. (2016) where we consider five sequential frames to compute the edge *(E)* and motion saliency *S* maps. They are computed using the Euclidean distance and the inter-image difference, respectively. Then, the combination of *E* and *S* is computed by applying the logical OR. This process extracts moving objects' contour, which will be used in the computation of different features.

The classification process consists of two steps that are feature extraction and label precision. As explained in Section 2, there exist several features in the literature. However, based on our benchmark study Honnit et al. (2018) and the most effective features for multi-classification were selected. These features are Centroid distance (CD), Central moment (CM), Zernike Moment (ZM), Fourier descriptor (FD), Histogram Oriented Gradient (HOG), Horizontal and Vertical Projection (HV-P), and Morphological features (MF) (i.e., anthropometry, compactness, solidity or convexity, aspect ratio). These extracted features are fed up to the used classifier in the next step.

Considering $p$ detected objects and $n$ features computed in step 1, a classification is conducted for each detected object using each feature separately which gives a $p\times n$matrix of probability of belonging $PB$ where $PB_{i,j}$ is the probability of belonging of the detected object $i$ using the feature $j$. Each element $p^k_{i,j}$in $PB_{i,j}$ is the probability of belonging of the detected object $i$ to the class $k$ using the feature $j$. Considering the $i^{th}$ detected object and its probability of belonging $PB_{i,j}\forall j\in n$, where:

$$PB_{i,j}=\left\{\begin{array}{c} class1:(p^1_{i,1},p^1_{i,2},\cdots,p^1_{i,n}),\\ class2:(p^2_{i,1},p^2_{i,2},\ldots,p^2_{i,n}),\\ \cdots,\\ classk:(p^k_{i,1},p^k_{i,2},\cdots,p^k_{i,n}) \end{array}\right\}. \quad (4)$$

The next operation consists on fusing the obtained probabilities for each feature and each detected object. Thus, all the possible pairs of $p^k_{i,j}$ are fused using the T-conorm operator (i.e., Section 3), called $item(i,k)$, where:

$$item(i,k)=max(T-conorm(p^k_{i,j},p^k_{i,l})),\forall i\in[1,p],\forall k \in[1,7],\forall j,l\in[1,n],j\neq l \quad (5)$$

The label of the $i^{th}$ detected object is the maximums of all the obtained items value. The computation procedure is shown in Fig. 2 and the pseudo-code is presented in Algorithm 1.

**Algorithm 1** Fusion of the obtained probabilities of belonging

```
n ← thenumberoftheusedfeatures
k ← thenumberoftheusedclasses
p ← thenumberofthedetectedobjects
for i = 1 : p
  maximumClass = 0
  winningClass = −1
  extract the n features
  for j = 1 : n
    Conduct a pre-classification
     Compute the posterior probability
   end for
   for d = 1 : k
     maximumItem = 0
     for j = 1 : n
     for l = 1 : n
       if j ≠ l
         value = T − conorm(p^d_{i,j}, p^d_{i,l})
        if value > maximum
       maximum = value
       winningClass = d
     end if
      end if
       end for
   end for
   if maximum > maximumClass
    maximumClass = maximum
    winningClass = d
    end if
  end for
  assign to the i^th object the winningClass
end for
```

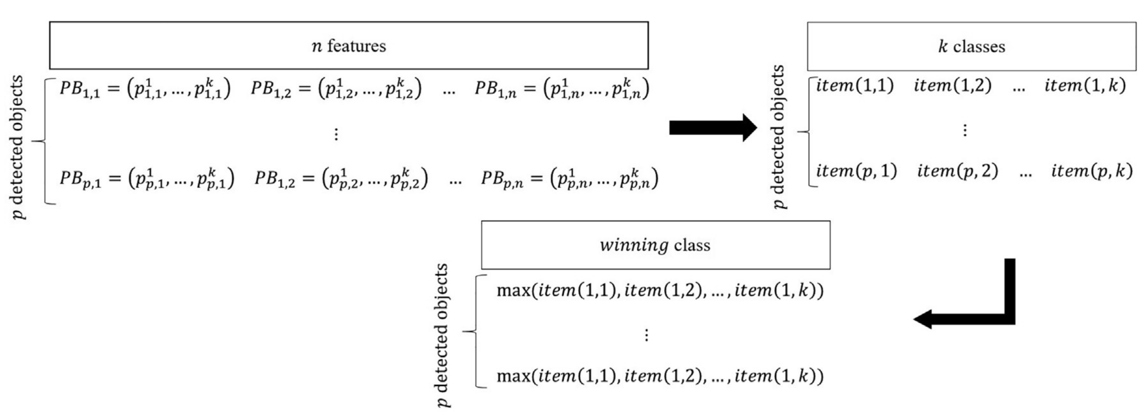


**Fig. 2.** Fusion procedure.

## 5. Experimental results

In our experimental study, we used two datasets, public (Dataset, 2014) *(D1)* and (UCF, 2018) *(D2)*. We selected eight categories from D1, where each one of them contains three videos. From D2, we used the normal videos category that contains forty-one videos. Samples of the used videos are shown in Fig. 3.

Moving objects were firstly detected and extracted from both datasets. Samples of the obtained results are shown in Fig. 4. The experiments were performed under a processor Intel(R) Core (TM) i7, CPU 2.81 GHZ and 12 RAM and using Matlab'16a.

In our experimental tests, we investigate two multi-classification classifiers Support Vector Machine (SVM) and K-Nearest Neighbor (KNN). They are known for their simplicity and high performance in video surveillance field. Their parameters were tuned using a basic genetic algorithm and they are shown in Table 2.

In order to evaluates the robustness of our approach we used different number of classes and features. The used classes in our experimental tests are:

- 3 classes *(3C)*: human (Hum), vehicle (Veh) and other;
- 5 classes *(5C)*: human (Hum), vehicle (Veh), other, human in a bicycle (HB) and group of objects (grpO);
- 7 classes *(7C)*: human (Hum), vehicle (Veh), group of human (grpH), human in a bicycle (HB), group of vehicles (grpV), group of objects (grpO) and other.

Based on the perceptual belonging of features, the following groups were constructed:

- 3 features *(3F)*: MF, HV-P, ZM;
- 5 features *(5F)*: H-VP, MF, ZM, HoG, CD;
- 7 features *(7C)*: H-VP, MF, ZM, HoG, CD, CM, FD.

### *5.1. Classical approach of classification*

As mentioned before the classical approach of moving object classification consists in using one or two features and one classifier. The obtained results are compared based on the classification accuracy rate *(CAR)*. The SVM classifier performs better than the KNN classifier FD, HoG, HV-P, and MF features. In contrary, the KNN classifier outperforms the SVM classifier when using CD, CM, and ZM features. This is explained by the nature of the used features. The common result between the SVM and KNN classifiers is that the classification accuracy decreases significantly when the number of classes increases. As can be seen in Tables 5 and 6, the ZM feature does not give a high accuracy compared to the other features when using D2 dataset.

### *5.2. Fusion approach*

In order to evaluate the performance of our model and to validate its robustness against the variation of the number of classes

(a) (b)

**Fig. 3.** Samples of the used videos. (a) public dataset2014. (b) UCF-Crime dataset.

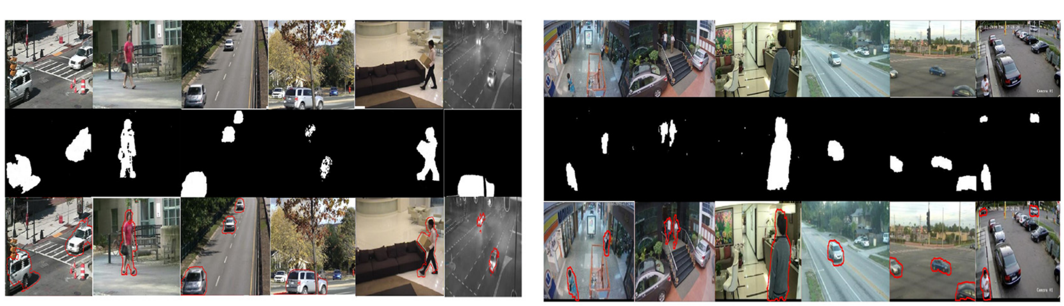

(a) (b)

**Fig. 4.** Samples of the obtained results using our hybrid approach for moving objects detection. (a) public dataset2014. (b) UCF-Crime dataset.

Please cite this article as: B. Honnit, K. B. Soulami, M. N. Saidi et al., Moving objects multi-classification based on information fusion, Journal of King Saud University –
Computer and Information Sciences, https://doi.org/10.1016/j.jksuci.2020.05.003

**Table 2**
The classifiers parameters.

| SVM | KNN |
|---|---|
| Kernel Function: polynomial<br>Polynomial order: 3<br>Kernel Scale: auto<br>Box Constraint: 1<br>Coding: one vs one | Distance: Euclidean<br>Number of Neighbors: 5<br>Distance weight: 1 |

and features, we conduct two experiments. In the first experiment, we fix the number of features and we variate the number of classes i.e., we compute the CAR for 3, 5, and 7 classes. In the second experiment, we fix the number of classes to five and we variate the number of features i.e., 3, 5, and 7 features. The first test aims we compare the performance of the classical fusion approach against our proposed approach using the accuracy metrics. While in the second test, we use the recall and precision metrics. They are defined as follows:

$$prescision = \frac{TP}{TP + FP} \quad \text{and} \quad recall = \frac{TP}{TP + FN}.$$

where $TP, FP, FN$ are, respectively, well classified objects of class k, well classified objects of other classes, wrongly classified objects of other classes. In the following, precision and recall will be symbolized by $P_{rcs}$ and $R_{cl}$.

**Test 1:** from analyzing Tables 7 and 8, we find that SVM shows a good performance than KNN. The used T-conorm operators outperform the other fusion methods (i.e., Section 3) with approximately 10% with the SVM classifier and 3% with the KNN classifier. In fact, Probabilistic and Luka operators show a high robustness against the increase of the number of classes, contrarily to Zadeh and Einstein, with a difference of 0.04%.

According to the giving results in Tables 9 and 10, our model shows approximately the same performance and results for both D1 and D2 datasets.

**Test 2:** as shown in Tables 11 and 12 the probabilistic operator could not classify objects of type Other when the number of classes is equal to three. The same type were not classified when the number of classes is equal to five and seven. Objects of type bicyHuman were not classified when using seven classes. This is explained by the fact that there is a confusion the pattern of bicyHuman with the pattern of a group of objects. However, our model shows a good performance compared to the other fusion techniques. The obtained results using the D2 dataset i.e., Tables 13 and 14 confirmed that our method emulates the other fusion approaches and prove that it is able to improve the classification results.

**Table 3**
CAR using SVM and D1.

| (%) | CD | CM | ZM | FD | HoG | HV-P | MF |
|---|---|---|---|---|---|---|---|
| 3C | 67.50 | 87 | 80 | 79 | 72 | 91.45 | 85 |
| 5C | 66.90 | 86.50 | 79 | 78 | 71 | 88 | 82 |
| 7C | 64.72 | 85 | 78 | 77 | 69.83 | 86 | 81.50 |

**Table 4**
CAR using KNN and D1.

| (%) | CD | CM | ZM | FD | HoG | HV-P | MF |
|---|---|---|---|---|---|---|---|
| 3C | 63.40 | 88.08 | 85.10 | 67.60 | 71.80 | 90.70 | 84.30 |
| 5C | 61.55 | 85 | 83.10 | 65.70 | 69.10 | 87.70 | 82.93 |
| 7C | 60.31 | 84 | 81.88 | 63.02 | 67.85 | 85.41 | 80.81 |

**Table 5**
CAR using SVM and D2.

| (%) | CD | CM | ZM | FD | HoG | HV-P | MF |
|---|---|---|---|---|---|---|---|
| 3C | 67.82 | 88.23 | 79 | 88 | 80 | 92 | 88 |
| 5C | 67.90 | 87 | 79 | 78 | 75 | 87.08 | 86 |
| 7C | 65.12 | 85.44 | 76 | 79.17 | 73 | 86 | 81.87 |

**Table 6**
CAR using KNN and D2.

| (%) | CD | CM | ZM | FD | HoG | HV-P | MF |
|---|---|---|---|---|---|---|---|
| 3C | 64 | 88 | 85.10 | 68 | 71 | 90.87 | 85 |
| 5C | 62.72 | 86.50 | 84 | 66 | 68.12 | 88 | 83 |
| 7C | 61 | 83 | 81.88 | 63.15 | 66 | 84 | 79 |

**Table 7**
CAR using SVM and D1.

| (%) | Mean | MV | T-conorm operators | | | |
|---|---|---|---|---|---|---|
| | | | Zadeh | Prob | Luka | Ein |
| 3C | 89.78 | 99.91 | 99.97 | 99.97 | 99.91 | 99.97 |
| 5C | 96.46 | 91.01 | 98.23 | 99.97 | 99.97 | 99.8 |
| 7C | 98.82 | 88.52 | 98.16 | 99.93 | 99.93 | 98.5 |

Please cite this article as: B. Honnit, K. B. Soulami, M. N. Saidi et al., Moving objects multi-classification based on information fusion, Journal of King Saud University –
Computer and Information Sciences, https://doi.org/10.1016/j.jksuci.2020.05.003

**Table 8**
CAR using KNN and D1.

| (%) | Mean | MV | T-conorm operators | | | |
|---|---|---|---|---|---|---|
| | | | Zadeh | Prob | Luka | Ein |
| 3C | 79.32 | 79.93 | 81.44 | 80.82 | 81.51 | 81.78 |
| 5C | 78.36 | 78.62 | 78.75 | 81.44 | 80.46 | 80.79 |
| 7C | 75.88 | 76.34 | 76.47 | 78.96 | 78.51 | 79.10 |

**Table 9**
CAR using SVM and D2.

| (%) | Mean | MV | T-conorm operators | | | |
|---|---|---|---|---|---|---|
| | | | Zadeh | Prob | Luka | Ein |
| 3C | 98 | 99.95 | 99 | 99.12 | 99.85 | 99.44 |
| 5C | 98 | 92.18 | 98.50 | 99 | 99.12 | 99 |
| 7C | 96 | 90.52 | 98.14 | 99 | 99 | 99 |

**Table 10**
CAR using KNN and D2.

| (%) | Mean | MV | T-conorm operators | | | |
|---|---|---|---|---|---|---|
| | | | Zadeh | Prob | Luka | Ein |
| 3C | 80.21 | 80.41 | 81.75 | 81.78 | 81.48 | 81.71 |
| 5C | 80 | 80.20 | 81.02 | 81.44 | 81 | 80.50 |
| 7C | 79 | 80 | 80 | 81 | 80 | 80 |

Moreover, KNN is unable to classify the other types except for objects of type human and vehicle.

The same test (test 2) is repeated using 5 features in order to evaluate the robustness of our model against a non-informative feature by using the centroid distance (CD) descriptor (Tables 3–6). Based on the presented results in Tables 15 and 16, we can note that all the methods have a problem to classify objects of type other either by the SVM classifier or the KNN classifier. While using

**Table 11**
$P_{rcs}$ and $R_{cl}$ of SVM using D1.

| SVM - 3C | | FMR | | T-conorm | | | |
|---|---|---|---|---|---|---|---|
| | | Mean | MV | Zadeh | Prob | Luka | Ein |
| Other | $P_{rcs}$ | 0.93 | 0.95 | 0.93 | 0.95 | 0.95 | 0.95 |
| | $R_{cl}$ | 0.77 | 0.95 | 0.77 | 0.95 | 0.95 | 0.95 |
| Hum | $P_{rcs}$ | 0.76 | 0.99 | 0.76 | 0.99 | 0.99 | 0.99 |
| | recall | 0.98 | 0.99 | 0.98 | 0.94 | 0.94 | 0.92 |
| Veh | $P_{rcs}$ | 0.80 | 0.95 | 0.80 | 0.92 | 0.91 | 0.95 |
| | $R_{cl}$ | 0.80 | 0.95 | 0.80 | 0.99 | 0.99 | 0.99 |
| SVM - 5C | | | | | | | |
| Other | $P_{rcs}$ | 0.85 | 0.85 | 0.85 | 0.85 | 0.85 | 0.85 |
| | $R_{cl}$ | 0.38 | 0.82 | 0.43 | 0.43 | 0.85 | 0.85 |
| HB | $P_{rcs}$ | 0.84 | 0.66 | 0.82 | 0.99 | 0.95 | 0.99 |
| | $R_{cl}$ | 0.6 | 0.5 | 0.91 | 0.91 | 0.99 | 0.95 |
| grpO | $P_{rcs}$ | 0.99 | 0.99 | 0.99 | 0.99 | 0.96 | 0.99 |
| | $R_{cl}$ | 0.99 | 0.98 | 0.99 | 0.93 | 0.99 | 0.95 |
| Hum | $P_{rcs}$ | 0.98 | 0.97 | 0.95 | 0.99 | 0.99 | 0.99 |
| | $R_{cl}$ | 0.99 | 0.98 | 0.98 | 0.98 | 0.97 | 0.94 |
| Veh | $P_{rcs}$ | 0.98 | 0.88 | 0.99 | 0.99 | 0.95 | 0.99 |
| | $R_{cl}$ | 0.99 | 0.99 | 0.99 | 0.99 | 0.99 | 0.91 |
| SVM - 7C | | | | | | | |
| Other | $P_{rcs}$ | 0.73 | 0.73 | 0.73 | 0.73 | 0.73 | 0.73 |
| | $R_{cl}$ | 0.73 | 0.73 | 0.73 | 0.73 | 0.73 | 0.73 |
| HB | $P_{rcs}$ | 0.73 | 0.82 | 0.82 | 0.95 | 0.96 | 0.96 |
| | $R_{cl}$ | 0.73 | 0.99 | 0.64 | 0.99 | 0.99 | 0.99 |
| grpH | $P_{rcs}$ | 0.99 | 0.99 | 0.83 | 0.99 | 0.99 | 0.99 |
| | $R_{cl}$ | 0.99 | 0.99 | 0.83 | 0.96 | 0.95 | 0.92 |
| grpO | $P_{rcs}$ | 0.89 | 0.99 | 0.99 | 0.99 | 0.99 | 0.99 |
| | $R_{cl}$ | 0.89 | 0.99 | 0.99 | 0.99 | 0.99 | 0.99 |
| grpV | $P_{rcs}$ | 0.89 | 0.78 | 0.68 | 0.84 | 0.86 | 0.84 |
| | $R_{cl}$ | 0.89 | 0.99 | 0.68 | 0.99 | 0.99 | 0.99 |
| Hum | $P_{rcs}$ | 0.99 | 0.99 | 0.95 | 0.99 | 0.99 | 0.99 |
| | $R_{cl}$ | 0.88 | 0.97 | 0.98 | 0.98 | 0.99 | 0.99 |
| Veh | $P_{rcs}$ | 0.99 | 0.99 | 0.89 | 0.96 | 0.99 | 0.99 |
| | $R_{cl}$ | 0.97 | 0.99 | 0.98 | 0.99 | 0.99 | 0.99 |

**Table 12**
$P_{rcs}$ and $R_{cl}$ of KNN using D1.

| KNN - 3C | | FMR | | T-conorm | | | |
|---|---|---|---|---|---|---|---|
| | | Mean | MV | Zadeh | Prob | Luka | Ein |
| Other | $P_{rcs}$ | 0.58 | 0.64 | 0.74 | 0.32 | 0.83 | 0.59 |
| | $R_{cl}$ | 0.58 | 0.64 | 0.79 | 0.32 | 0.83 | 0.59 |
| Hum | $P_{rcs}$ | 0.92 | 0.94 | 0.92 | 0.9 | 0.92 | 0.91 |
| | $R_{cl}$ | 0.78 | 0.79 | 0.82 | 0.84 | 0.82 | 0.83 |
| Veh | $P_{rcs}$ | 0.77 | 0.77 | 0.83 | 0.79 | 0.83 | 0.84 |
| | $R_{cl}$ | 0.83 | 0.84 | 0.82 | 0.83 | 0.82 | 0.82 |
| KNN - 5C | | | | | | | |
| Other | $P_{rcs}$ | 0.23 | 0.23 | 0.23 | 0.23 | 0.23 | 0.23 |
| | $R_{cl}$ | 0.23 | 0.23 | 0.23 | 0.23 | 0.23 | 0.23 |
| HB | $P_{rcs}$ | 0.9 | 0.69 | 0.9 | 0.8 | 0.9 | 0.67 |
| | $R_{cl}$ | 0.65 | 0.63 | 0.68 | 0.89 | 0.67 | 0.95 |
| grpO | $P_{rcs}$ | 0.98 | 0.97 | 0.97 | 0.99 | 0.99 | 0.99 |
| | $R_{cl}$ | 0.99 | 0.99 | 0.99 | 0.99 | 0.99 | 0.99 |
| Hum | $P_{rcs}$ | 0.89 | 0.86 | 0.9 | 0.92 | 0.87 | 0.92 |
| | $R_{cl}$ | 0.78 | 0.82 | 0.78 | 0.81 | 0.83 | 0.8 |
| Veh | $P_{rcs}$ | 0.78 | 0.79 | 0.78 | 0.83 | 0.85 | 0.83 |
| | $R_{cl}$ | 0.92 | 0.93 | 0.92 | 0.92 | 0.92 | 0.9 |
| KNN - 7C | | | | | | | |
| Other | $P_{rcs}$ | 0.28 | 0.28 | 0.63 | 0.28 | 0.99 | 0.28 |
| | $R_{cl}$ | 0.28 | 0.28 | 0.63 | 0.28 | 0.99 | 0.28 |
| HB | $P_{rcs}$ | 0.9 | 0.9 | 0.69 | 0.67 | 0.9 | 0.67 |
| | $R_{cl}$ | 0.72 | 0.7 | 0.62 | 0.98 | 0.69 | 0.98 |
| grpH | $P_{rcs}$ | 0.5 | 0.33 | 0.83 | 0.33 | 0.67 | 0.33 |
| | $R_{cl}$ | 0.99 | 0.99 | 0.31 | 0.99 | 0.99 | 0.99 |
| grpO | $P_{rcs}$ | 0.98 | 0.97 | 0.33 | 0.99 | 0.99 | 0.99 |
| | $R_{cl}$ | 0.99 | 0.99 | 0.33 | 0.99 | 0.99 | 0.99 |
| grpV | $P_{rcs}$ | 0.3 | 0.27 | 0.27 | 0.24 | 0.3 | 0.24 |
| | $R_{cl}$ | 0.31 | 0.34 | 0.31 | 0.38 | 0.37 | 0.39 |
| Hum | $P_{rcs}$ | 0.89 | 0.9 | 0.87 | 0.92 | 0.88 | 0.92 |
| | $R_{cl}$ | 0.78 | 0.78 | 0.84 | 0.81 | 0.83 | 0.81 |
| Veh | $P_{rcs}$ | 0.73 | 0.75 | 0.76 | 0.83 | 0.82 | 0.83 |
| | $R_{cl}$ | 0.78 | 0.79 | 0.82 | 0.78 | 0.78 | 0.78 |

**Table 13**
$P_{rcs}$ and $R_{cl}$ of SVM using D2.

| SVM - 3C | | FMR | | T-conorm | | | |
|---|---|---|---|---|---|---|---|
| | | Mean | MV | Zadeh | Prob | Luka | Ein |
| Other | $P_{rcs}$ | 0.85 | 0.85 | 0.98 | 0.98 | 0.85 | 0.85 |
| | $R_{cl}$ | 0.85 | 0.85 | 0.95 | 0.95 | 0.85 | 0.85 |
| Hum | $P_{rcs}$ | 0.76 | 0.94 | 0.76 | 0.99 | 0.99 | 0.99 |
| | $R_{cl}$ | 0.98 | 0.93 | 0.98 | 0.94 | 0.94 | 0.92 |
| Veh | $P_{rcs}$ | 0.80 | 0.94 | 0.80 | 0.92 | 0.95 | 0.95 |
| | $R_{cl}$ | 0.80 | 0.93 | 0.80 | 0.99 | 0.99 | 0.99 |
| SVM - 5C | | | | | | | |
| Other | $P_{rcs}$ | 0.93 | 0.95 | 0.95 | 0.95 | 0.95 | 0.95 |
| | $R_{cl}$ | 0.77 | 0.95 | 0.94 | 0.95 | 0.95 | 0.95 |
| HB | $P_{rcs}$ | 0.93 | 0.95 | 0.95 | 0.94 | 0.95 | 0.94 |
| | $R_{cl}$ | 0.77 | 0.95 | 0.94 | 0.93 | 0.95 | 0.93 |
| grpO | $P_{rcs}$ | 0.76 | 0.76 | 0.95 | 0.95 | 0.95 | 0.94 |
| | $R_{cl}$ | 0.77 | 0.77 | 0.94 | 0.93 | 0.95 | 0.94 |
| Hum | $P_{rcs}$ | 0.90 | 0.97 | 0.95 | 0.99 | 0.99 | 0.99 |
| | $R_{cl}$ | 0.91 | 0.98 | 0.98 | 0.98 | 0.97 | 0.94 |
| Veh | $P_{rcs}$ | 0.92 | 0.88 | 0.99 | 0.99 | 0.95 | 0.99 |
| | $R_{cl}$ | 0.90 | 0.90 | 0.99 | 0.99 | 0.99 | 0.91 |
| SVM - 7C | | | | | | | |
| Other | $P_{rcs}$ | 0.74 | 0.74 | 0.95 | 0.95 | 0.95 | 0.98 |
| | $R_{cl}$ | 0.73 | 0.73 | 0.97 | 0.96 | 0.97 | 0.99 |
| HB | $P_{rcs}$ | 0.73 | 0.82 | 0.95 | 0.95 | 0.96 | 0.96 |
| | $R_{cl}$ | 0.73 | 0.79 | 0.95 | 0.99 | 0.99 | 0.99 |
| grpH | $P_{rcs}$ | 0.89 | 0.82 | 0.97 | 0.99 | 0.99 | 0.99 |
| | $R_{cl}$ | 0.91 | 0.79 | 0.97 | 0.96 | 0.99 | 0.94 |
| grpO | $P_{rcs}$ | 0.89 | 0.82 | 0.99 | 0.99 | 0.99 | 0.99 |
| | $R_{cl}$ | 0.89 | 0.79 | 0.99 | 0.99 | 0.99 | 0.99 |
| grpV | $P_{rcs}$ | 0.89 | 0.82 | 0.97 | 0.84 | 0.99 | 0.97 |
| | $R_{cl}$ | 0.89 | 0.79 | 0.97 | 0.99 | 0.99 | 0.99 |
| Hum | $P_{rcs}$ | 0.89 | 0.82 | 0.95 | 0.99 | 0.99 | 0.99 |
| | $R_{cl}$ | 0.91 | 0.79 | 0.98 | 0.98 | 0.99 | 0.99 |
| Veh | $P_{rcs}$ | 0.89 | 0.82 | 0.99 | 0.96 | 0.99 | 0.99 |
| | $R_{cl}$ | 0.89 | 0.79 | 0.98 | 0.99 | 0.99 | 0.99 |

Please cite this article as: B. Honnit, K. B. Soulami, M. N. Saidi et al., Moving objects multi-classification based on information fusion, Journal of King Saud University –
Computer and Information Sciences, https://doi.org/10.1016/j.jksuci.2020.05.003

**Table 14**
$P_{rcs}$ and $R_{cl}$ of KNN using D2.

| KNN - 3C | | FMR | | T-conorm | | | |
|---|---|---|---|---|---|---|---|
| | | Mean | MV | Zadeh | Prob | Luka | Ein |
| Other | $P_{rcs}$ | 0.583 | 0.640 | 0.742 | 0.325 | 0.831 | 0.594 |
| | $R_{cl}$ | 0.583 | 0.635 | 0.793 | 0.322 | 0.834 | 0.594 |
| Hum | $P_{rcs}$ | 0.924 | 0.945 | 0.926 | 0.926 | 0.923 | 0.915 |
| | $R_{cl}$ | 0.785 | 0.789 | 0.825 | 0.843 | 0.824 | 0.842 |
| Veh | $P_{rcs}$ | 0.772 | 0.774 | 0.837 | 0.793 | 0.833 | 0.841 |
| | $R_{cl}$ | 0.834 | 0.842 | 0.825 | 0.831 | 0.820 | 0.824 |
| KNN - 5C | | | | | | | |
| Other | $P_{rcs}$ | 0.333 | 0.233 | 0.234 | 0.230 | 0.230 | 0.230 |
| | $R_{cl}$ | 0.331 | 0.234 | 0.234 | 0.233 | 0.230 | 0.241 |
| HB | $P_{rcs}$ | 0.901 | 0.692 | 0.901 | 0.803 | 0.901 | 0.672 |
| | $R_{cl}$ | 0.650 | 0.635 | 0.681 | 0.891 | 0.672 | 0.953 |
| grpO | $P_{rcs}$ | 0.984 | 0.973 | 0.973 | 0.990 | 0.993 | 0.994 |
| | $R_{cl}$ | 0.991 | 0.990 | 0.992 | 0.990 | 0.992 | 0.992 |
| Hum | $P_{rcs}$ | 0.893 | 0.864 | 0.902 | 0.924 | 0.871 | 0.921 |
| | $R_{cl}$ | 0.784 | 0.825 | 0.783 | 0.812 | 0.833 | 0.804 |
| Veh | $P_{rcs}$ | 0.783 | 0.791 | 0.781 | 0.831 | 0.854 | 0.834 |
| | $R_{cl}$ | 0.924 | 0.932 | 0.924 | 0.924 | 0.925 | 0.903 |
| KNN - 7C | | | | | | | |
| Other | $P_{rcs}$ | 0.285 | 0.284 | 0.633 | 0.285 | 0.992 | 0.285 |
| | $R_{cl}$ | 0.285 | 0.283 | 0.633 | 0.285 | 0.991 | 0.283 |
| HB | $P_{rcs}$ | 0.904 | 0.903 | 0.692 | 0.674 | 0.904 | 0.673 |
| | $R_{cl}$ | 0.723 | 0.705 | 0.624 | 0.984 | 0.695 | 0.985 |
| grpH | $P_{rcs}$ | 0.506 | 0.334 | 0.835 | 0.338 | 0.674 | 0.334 |
| | $R_{cl}$ | 0.993 | 0.994 | 0.313 | 0.995 | 0.993 | 0.994 |
| grpO | $P_{rcs}$ | 0.985 | 0.973 | 0.334 | 0.994 | 0.995 | 0.993 |
| | $R_{cl}$ | 0.993 | 0.998 | 0.335 | 0.994 | 0.993 | 0.994 |
| grpV | $P_{rcs}$ | 0.304 | 0.275 | 0.273 | 0.244 | 0.307 | 0.245 |
| | $R_{cl}$ | 0.313 | 0.344 | 0.312 | 0.383 | 0.369 | 0.395 |
| Hum | $P_{rcs}$ | 0.893 | 0.902 | 0.874 | 0.925 | 0.885 | 0.924 |
| | $R_{cl}$ | 0.784 | 0.783 | 0.844 | 0.815 | 0.834 | 0.815 |
| Veh | $P_{rcs}$ | 0.734 | 0.754 | 0.764 | 0.835 | 0.825 | 0.835 |
| | $R_{cl}$ | 0.784 | 0.793 | 0.824 | 0.784 | 0.874 | 0.783 |

**Table 15**
$P_{rcs}$ & $R_{cl}$ of SVM using D1.

| SVM - 3C | | FMR | | T-conorm | | | |
|---|---|---|---|---|---|---|---|
| | | Mean | MV | Zadeh | Prob | Luka | Ein |
| Other | $P_{rcs}$ | 0.94 | 0.95 | 0.93 | 0.95 | 0.95 | 0.95 |
| | $R_{cl}$ | 0.79 | 0.88 | 0.77 | 0.92 | 0.88 | 0.95 |
| Hum | $P_{rcs}$ | 0.76 | 0.99 | 0.76 | 0.99 | 0.99 | 0.99 |
| | $R_{cl}$ | 0.99 | 0.99 | 0.98 | 0.99 | 0.99 | 0.99 |
| Veh | $P_{rcs}$ | 0.79 | 0.995 | 0.8 | 0.99 | 0.99 | 0.99 |
| | $R_{cl}$ | 0.79 | 0.995 | 0.8 | 0.99 | 0.99 | 0.99 |
| SVM - 5C | | | | | | | |
| Other | $P_{rcs}$ | 0.85 | 0.85 | 0.85 | 0.85 | 0.85 | 0.85 |
| | $R_{cl}$ | 0.39 | 0.82 | 0.42 | 0.43 | 0.82 | 0.8 |
| HB | $P_{rcs}$ | 0.84 | 0 | 0.82 | 0.99 | 0.99 | 0.99 |
| | $R_{cl}$ | 0.62 | 0 | 0.91 | 0.99 | 0.99 | 0.99 |
| grpO | $P_{rcs}$ | 0.99 | 0 | 0.99 | 0.99 | 0.99 | 0.99 |
| | $R_{cl}$ | 0.99 | 0 | 0.5 | 0.99 | 0.99 | 0.99 |
| Hum | $P_{rcs}$ | 0.98 | 0.99 | 0.96 | 0.99 | 0.99 | 0.99 |
| | $R_{cl}$ | 0.98 | 0.91 | 0.98 | 0.99 | 0.99 | 0.99 |
| Veh | $P_{rcs}$ | 0.98 | 0.99 | 0.99 | 0.99 | 0.99 | 0.99 |
| | $R_{cl}$ | 0.99 | 0.99 | 0.99 | 0.99 | 0.99 | 0.99 |
| SVM - 7C | | | | | | | |
| Other | $P_{rcs}$ | 0.5 | 0.5 | 0.67 | 0.99 | 0.99 | 0.99 |
| | $R_{cl}$ | 0.44 | 0.5 | 0.77 | 0.99 | 0.99 | 0.99 |
| HB | $P_{rcs}$ | 0.98 | 0 | 0.35 | 0.99 | 0.99 | 0.99 |
| | $R_{cl}$ | 0.99 | 0 | 0.23 | 0.99 | 0.99 | 0.99 |
| grpH | $P_{rcs}$ | 0 | 0 | 0.99 | 0.99 | 0.99 | 0.35 |
| | $R_{cl}$ | 0 | 0 | 0.99 | 0.99 | 0.99 | 0.23 |
| grpO | $P_{rcs}$ | 0.99 | 0 | 0.17 | 0.99 | 0.99 | 0.99 |
| | $R_{cl}$ | 0.99 | 0 | 0.19 | 0.99 | 0.99 | 0.99 |
| grpV | $P_{rcs}$ | 0.68 | 0.89 | 0.89 | 0.97 | 0.97 | 0.81 |
| | $R_{cl}$ | 0.5 | 0.99 | 0.99 | 0.99 | 0.99 | 0.99 |
| Hum | $P_{rcs}$ | 0.99 | 0.99 | 0.87 | 0.99 | 0.99 | 0.99 |
| | $R_{cl}$ | 0.97 | 0.87 | 0.67 | 0.99 | 0.99 | 0.98 |
| Veh | $P_{rcs}$ | 0.99 | 0.99 | 0.89 | 0.96 | 0.99 | 0.99 |
| | $R_{cl}$ | 0.97 | 0.99 | 0.98 | 0.99 | 0.99 | 0.99 |

Please cite this article as: B. Honnit, K. B. Soulami, M. N. Saidi et al., Moving objects multi-classification based on information fusion, Journal of King Saud University –
Computer and Information Sciences, https://doi.org/10.1016/j.jksuci.2020.05.003

**Table 16**
$P_{rcs}$ & $R_{cl}$ of KNN using D1.

| KNN - 3C | | FMR | | T-conorm | | | |
|---|---|---|---|---|---|---|---|
| | | Mean | MV | Zadeh | Prob | Luka | Ein |
| Other | $P_{rcs}$ | 0.21 | 0.21 | 0.21 | 0.21 | 0.21 | 0.21 |
| | $R_{cl}$ | 0.41 | 0.18 | 0.14 | 0.23 | 0.57 | 0.55 |
| Hum | $P_{rcs}$ | 0.92 | 0.87 | 0.63 | 0.89 | 0.92 | 0.94 |
| | $R_{cl}$ | 0.8 | 0.78 | 0.7 | 0.83 | 0.82 | 0.82 |
| Veh | $P_{rcs}$ | 0.75 | 0.687 | 0.64 | 0.78 | 0.82 | 0.82 |
| | $R_{cl}$ | 0.82 | 0.822 | 0.63 | 0.83 | 0.82 | 0.84 |
| KNN - 5C | | | | | | | |
| Other | $P_{rcs}$ | 0.28 | 0.28 | 0.28 | 0.28 | 0.28 | 0.28 |
| | $R_{cl}$ | 0.06 | 0.04 | 0.06 | 0.06 | 0 | 0 |
| HB | $P_{rcs}$ | 0.9 | 0.52 | 0.31 | 0.51 | 0.52 | 0.51 |
| | $R_{cl}$ | 0.71 | 0.94 | 0.31 | 0.99 | 0.99 | 0.99 |
| grpO | $P_{rcs}$ | 0.25 | 0.25 | 0.5 | 0.3 | 0.3 | 0.3 |
| | $R_{cl}$ | 0.5 | 0.5 | 0.4 | 0.5 | 0.5 | 0.5 |
| Hum | $P_{rcs}$ | 0.87 | 0.88 | 0.55 | 0.92 | 0.9 | 0.9 |
| | $R_{cl}$ | 0.78 | 0.77 | 0.58 | 0.8 | 0.81 | 0.8 |
| Veh | $P_{rcs}$ | 0.78 | 0.73 | 0.51 | 0.79 | 0.8 | 0.8 |
| | $R_{cl}$ | 0.91 | 0.95 | 0.65 | 0.95 | 0.95 | 0.94 |
| KNN - 7C | | | | | | | |
| Other | $P_{rcs}$ | 0.5 | 0.5 | 0.8 | 0.8 | 0.8 | 0.75 |
| | $R_{cl}$ | 0.5 | 0.6 | 0.93 | 0.95 | 0.95 | 0.9 |
| HB | $P_{rcs}$ | 0.9 | 0.9 | 0.41 | 0.9 | 0.52 | 0.52 |
| | $R_{cl}$ | 0.71 | 0.73 | 0.35 | 0.71 | 0.97 | 0.97 |
| grpH | $P_{rcs}$ | 0.17 | 0.5 | 0.5 | 0.17 | 0.17 | 0 |
| | $R_{cl}$ | 0.19 | 0.31 | 0.4 | 0.23 | 0.27 | 0 |
| grpO | $P_{rcs}$ | 0 | 0.25 | 0.5 | 0 | 0 | 0 |
| | $R_{cl}$ | 0 | 0.25 | 0.5 | 0 | 0 | 0 |
| grpV | $P_{rcs}$ | 0.16 | 0.3 | 0.24 | 0.28 | 0.49 | 0.3 |
| | $R_{cl}$ | 0.35 | 0.31 | 0.18 | 0.35 | 0.55 | 0.6 |
| Hum | $P_{rcs}$ | 0.86 | 0.89 | 0.56 | 0.84 | 0.89 | 0.89 |
| | $R_{cl}$ | 0.79 | 0.78 | 0.61 | 0.84 | 0.82 | 0.82 |
| Veh | $P_{rcs}$ | 0.72 | 0.73 | 0.49 | 0.79 | 0.8 | 0.8 |
| | $R_{cl}$ | 0.8 | 0.78 | 0.59 | 0.79 | 0.77 | 0.77 |

**Table 17**
$P_{rcs}$ & $R_{cl}$ of SVM using D2.

| SVM - 3C | | FMR | | T-conorm | | | |
|---|---|---|---|---|---|---|---|
| | | Mean | MV | Zadeh | Prob | Luka | Ein |
| Other | $P_{rcs}$ | 0.90 | 0.91 | 0.99 | 0.99 | 0.92 | 0.99 |
| | $R_{cl}$ | 0.91 | 0.92 | 0.98 | 0.98 | 0.93 | 0.85 |
| Hum | $P_{rcs}$ | 0.90 | 0.97 | 0.98 | 0.99 | 0.99 | 0.99 |
| | $R_{cl}$ | 0.91 | 0.98 | 0.99 | 0.98 | 0.98 | 0.94 |
| Veh | $P_{rcs}$ | 0.92 | 0.90 | 0.99 | 0.99 | 0.98 | 0.99 |
| | $R_{cl}$ | 0.90 | 0.91 | 0.99 | 0.99 | 0.99 | 0.95 |
| SVM - 5C | | | | | | | |
| Other | $P_{rcs}$ | 0.95 | 0.95 | 0.97 | 0.97 | 0.97 | 0.97 |
| | $R_{cl}$ | 0.90 | 0.95 | 0.96 | 0.96 | 0.99 | 0.96 |
| HB | $P_{rcs}$ | 0.95 | 0.95 | 0.96 | 0.95 | 0.95 | 0.95 |
| | $R_{cl}$ | 0.90 | 0.95 | 0.96 | 0.96 | 0.98 | 0.96 |
| grpO | $P_{rcs}$ | 0.90 | 0.95 | 0.97 | 0.95 | 0.98 | 0.95 |
| | $R_{cl}$ | 0.95 | 0.95 | 0.96 | 0.99 | 0.99 | 0.99 |
| Hum | $P_{rcs}$ | 0.871 | 0.882 | 0.551 | 0.920 | 0.900 | 0.900 |
| | $R_{cl}$ | 0.98 | 0.95 | 0.98 | 0.98 | 0.96 | 0.98 |
| Veh | $P_{rcs}$ | 0.95 | 0.94 | 0.95 | 0.99 | 0.97 | 0.99 |
| | $R_{cl}$ | 0.90 | 0.95 | 0.95 | 0.99 | 0.99 | 0.99 |
| SVM - 7C | | | | | | | |
| Other | $P_{rcs}$ | 0.90 | 0.90 | 0.98 | 0.96 | 0.98 | 0.98 |
| | $R_{cl}$ | 0.89 | 0.89 | 0.99 | 0.97 | 0.99 | 0.99 |
| HB | $P_{rcs}$ | 0.85 | 0.85 | 0.97 | 0.98 | 0.98 | 0.96 |
| | $R_{cl}$ | 0.86 | 0.86 | 0.98 | 0.99 | 0.99 | 0.99 |
| grpH | $P_{rcs}$ | 0.90 | 0.90 | 0.99 | 0.99 | 0.99 | 0.99 |
| | $R_{cl}$ | 0.91 | 0.85 | 0.99 | 0.96 | 0.99 | 0.95 |
| grpO | $P_{rcs}$ | 0.90 | 0.90 | 0.99 | 0.99 | 0.99 | 0.99 |
| | $R_{cl}$ | 0.91 | 0.88 | 0.99 | 0.99 | 0.99 | 0.99 |
| grpV | $P_{rcs}$ | 0.92 | 0.93 | 0.98 | 0.96 | 0.99 | 0.97 |
| | $R_{cl}$ | 0.93 | 0.94 | 0.98 | 0.99 | 0.99 | 0.99 |
| Hum | $P_{rcs}$ | 0.92 | 0.93 | 0.98 | 0.99 | 0.99 | 0.99 |
| | $R_{cl}$ | 0.93 | 0.94 | 0.98 | 0.98 | 0.99 | 0.99 |
| Veh | $P_{rcs}$ | 0.92 | 0.91 | 0.99 | 0.96 | 0.99 | 0.99 |
| | $R_{cl}$ | 0.93 | 0.93 | 0.98 | 0.99 | 0.99 | 0.99 |

Please cite this article as: B. Honnit, K. B. Soulami, M. N. Saidi et al., Moving objects multi-classification based on information fusion, Journal of King Saud University –
Computer and Information Sciences, https://doi.org/10.1016/j.jksuci.2020.05.003

**Table 18**
$P_{rcs}$ & $R_{cl}$ of KNN using D2.

| KNN - 3C | | FMR | | T-conorm | | | |
|---|---|---|---|---|---|---|---|
| | | Mean | MV | Zadeh | Prob | Luka | Ein |
| Other | $P_{rcs}$ | 0.210 | 0.210 | 0.210 | 0.210 | 0.210 | 0.210 |
| | $R_{cl}$ | 0.410 | 0.180 | 0.141 | 0.231 | 0.572 | 0.551 |
| Hum | $P_{rcs}$ | 0.921 | 0.873 | 0.630 | 0.890 | 0.922 | 0.942 |
| | $R_{cl}$ | 0.803 | 0.782 | 0.703 | 0.831 | 0.822 | 0.821 |
| Veh | $P_{rcs}$ | 0.750 | 0.687 | 0.640 | 0.780 | 0.820 | 0.822 |
| | $R_{cl}$ | 0.820 | 0.822 | 0.630 | 0.830 | 0.822 | 0.843 |
| KNN - 5C | | | | | | | |
| Other | $P_{rcs}$ | 0.280 | 0.281 | 0.281 | 0.281 | 0.281 | 0.281 |
| | $R_{cl}$ | 0.060 | 0.041 | 0.063 | 0.063 | 0.041 | 0.031 |
| HB | $P_{rcs}$ | 0.901 | 0.523 | 0.310 | 0.510 | 0.520 | 0.510 |
| | $R_{cl}$ | 0.712 | 0.940 | 0.311 | 0.990 | 0.990 | 0.990 |
| grpO | $P_{rcs}$ | 0.250 | 0.251 | 0.500 | 0.300 | 0.303 | 0.303 |
| | $R_{cl}$ | 0.500 | 0.501 | 0.402 | 0.501 | 0.502 | 0.501 |
| Hum | $P_{rcs}$ | 0.871 | 0.882 | 0.551 | 0.920 | 0.900 | 0.900 |
| | $R_{cl}$ | 0.782 | 0.770 | 0.582 | 0.803 | 0.810 | 0.803 |
| Veh | $P_{rcs}$ | 0.782 | 0.730 | 0.510 | 0.790 | 0.803 | 0.803 |
| | $R_{cl}$ | 0.911 | 0.952 | 0.650 | 0.952 | 0.950 | 0.941 |
| KNN - 7C | | | | | | | |
| Other | $P_{rcs}$ | 0.502 | 0.503 | 0.800 | 0.800 | 0.800 | 0.750 |
| | $R_{cl}$ | 0.501 | 0.603 | 0.930 | 0.950 | 0.950 | 0.900 |
| HB | $P_{rcs}$ | 0.902 | 0.903 | 0.410 | 0.900 | 0.520 | 0.520 |
| | $R_{cl}$ | 0.710 | 0.731 | 0.350 | 0.710 | 0.970 | 0.970 |
| grpH | $P_{rcs}$ | 0.171 | 0.504 | 0.500 | 0.170 | 0.170 | 0.102 |
| | $R_{cl}$ | 0.191 | 0.313 | 0.400 | 0.230 | 0.270 | 0.113 |
| grpO | $P_{rcs}$ | 0.020 | 0.255 | 0.500 | 0.102 | 0.210 | 0.143 |
| | $R_{cl}$ | 0.034 | 0.254 | 0.500 | 0.004 | 0.210 | 0.241 |
| grpV | $P_{rcs}$ | 0.164 | 0.303 | 0.240 | 0.280 | 0.490 | 0.3001 |
| | $R_{cl}$ | 0.350 | 0.310 | 0.180 | 0.350 | 0.550 | 0.600 |
| Hum | $P_{rcs}$ | 0.860 | 0.892 | 0.560 | 0.840 | 0.890 | 0.890 |
| | $R_{cl}$ | 0.792 | 0.781 | 0.611 | 0.840 | 0.820 | 0.820 |
| Veh | $P_{rcs}$ | 0.722 | 0.732 | 0.492 | 0.790 | 0.800 | 0.800 |
| | $R_{cl}$ | 0.803 | 0.781 | 0.592 | 0.790 | 0.770 | 0.770 |

the SVM and 5 classes, contrarily to KNN, majority vote could not classify objects of type BicyHuman and a group of objects. All the methods using KNN were unable to classify objects of type group of objects except Zadeh operator. Moreover, Einstein did not classify objects of type grpHuman. However, the use of a non-informative feature did not influence the good performance of our model. But in the same time, the classification process shows better results when several features are used. Tables 17 and 18, show that our model is stable, since the obtained results are coherent. Contrarily to D1, our model was able to classify all the classes when using D2. The tests 2 was repeated using 7 features and the model showed the same performance.

## 6. Discussion

In our study, we aim to evaluate the performance of our model and its ability to improve the classification accuracy. At first, Tables 3–6, show that using only one feature, is not sufficient since a feature can be relevant and helps detecting an object but may fail in recognizing others. To solve this problem, the first proposed solution in the literature was based on combining several features. This approach is able to improve the classification accuracy. However, this combination results in a high dimensional matrix, which need a preprocession and demand a high execution time.

The second solution consists in using the majority vote and the mean rules fusion methods. These approaches are able to improve the classification performance. However, they are sensitive to some object's types (i.e., grpV, grpH, HB), and to the degree of reliability of the used features. In addition, the classification accuracy is decreased significantly when using a non-informative features, since both of them use the classifier's output directly.

In order to overcome the aforementioned problems, in our model we combine the posterior probabilities using the T-conorm operator before making the final decision. The presented results in Section 5 show that our method is robust against the less informative features and to the variation of the used number of classes and features. Moreover, it is able to improve the classification performance.

## 7. Conclusion

Moving object classification has an important role in video surveillance system. However, it is sensitive to the used features and number of classes. To solve this problem, researchers proposed the use of several features with a feature selection method. Others introduced new features and most of them used the binary classification. However, they have several limitations. Therefore, we propose in this paper a new model based on data fusion able to improve the classification accuracy.

At first, features are extracted and a pre-classification is conducted using each feature separately. These step allows the computation of the posterior probabilities. Then, the obtained probabilities are combined using the T-conorm operator. At last, the final decision is made by calculating the maximum.

Our model was evaluated using two datasets and compared with three methods: method based on combining features before the classification, the majority vote rule, and mean rule method. According to the obtained results, our model is able to improved the classification accuracy.

As for future work we aim to test our model in a real-time constraint using one camera. furthermore, it will be improved for a video surveillance system using several cameras.

Please cite this article as: B. Honnit, K. B. Soulami, M. N. Saidi et al., Moving objects multi-classification based on information fusion, Journal of King Saud University –
Computer and Information Sciences, https://doi.org/10.1016/j.jksuci.2020.05.003

## Declaration of Competing Interest

The authors declare that they have no known competing financial interests or personal relationships that could have appeared to influence the work reported in this paper.

## References

Al Jarouf, Y.A., Kurdy, M.-B., 2018. A hybrid method to detect and verify vehicle crash with haar-like features and svm over the web. 2018 International Conference on Computer and Applications (ICCA). IEEE, pp. 177–182.
Alamgir, N., Nguyen, K., Chandran, V., Boles, W., 2018. Combining multi-channel color space with local binary co-occurrence feature descriptors for accurate smoke detection from surveillance videos. Fire Safety J. 102, 1–10.
Avola, D., Bernardi, M., Foresti, G.L., 2019. Fusing depth and colour information for human action recognition. Multimedia Tools Appl. 78, 5919–5939.
Bogomolov, Y., Dror, G., Lapchev, S., Rivlin, E., Rudzsky, M., 2003. Classification of moving targets based on motion and appearance. BMVC, pp. 1–10.
Chapman, A.B., Peterson, K.S., Alba, P.R., DuVall, S.L., Patterson, O.V., 2019. Detecting adverse drug events with rapidly trained classification models. Drug Safety 42, 147–156.
Chen, J., Li, K., Deng, Q., Li, K., Philip, S.Y., 2019. Distributed deep learning model for intelligent video surveillance systems with edge computing. IEEE Trans. Industr. Inf.
Cheng, H., Sawhney, H.S., Divakaran, A., Yu, Q., Liu, J., Tamrakar, A., Ali, S., Javed, O., 2019. Classification, search and retrieval of complex video events. US Patent App. 10/198,509..
Cui, Y., Xu, H., Wu, J., Sun, Y., Zhao, J., 2019. Automatic vehicle tracking with roadside lidar data for the connected-vehicles system. IEEE Intell. Syst.
Dataset 2014 (2014). Dataset 2014. http://www.changedetection.net..
Honnit, B., Saidi, M.N., Tamtaoui, A., 2016. Hybrid approach for moving object detection. In: International Symposium on Ubiquitous Networking. Springer, pp. 481–489.
Honnit, B., Saidi, M.N., Tamtaoui, A., 2018. Experimental study: Influence of feature extraction in objects multiclassification. 2018 IEEE International Conference on Technology Management, Operations and Decisions (ICTMOD). IEEE, pp. 237–243.
Ikizler-Cinbis, N., Sclaroff, S., 2010. Object, scene and actions: Combining multiple features for human action recognition. In: European conference on computer vision. Springer, pp. 494–507.
Jabri, S., Saidallah, M., el Alaoui, A. e. B., El Fergougui, A., 2018. Moving vehicle detection using haar-like, lbp and a machine learning adaboost algorithm. 2018 IEEE International Conference on Image Processing, Applications and Systems (IPAS). IEEE, pp. 121–124.
Jemilda, G., Baulkani, S., 2018. Moving object detection and tracking using genetic algorithm enabled extreme learning machine. Int. J. Computers, Commun. Control 13.
Karthikeswaran, D., Sengottaiyan, N., Anbukaruppusamy, S., 2019. Video surveillance system against anti-terrorism by using adaptive linear activity classification (alac) technique. J. Med. Syst. 43, 256.
Kwan, C., Chou, B., Yang, J., Tran, T., 2019. Target tracking and classification directly in compressive measurement for low quality videos. In: Pattern Recognition and Tracking XXX (p. 1099505). International Society for Optics and Photonics volume 10995..
Laopracha, N., Sunat, K., Chiewchanwattana, S., 2019. A novel feature selection in vehicle detection through the selection of dominant patterns of histograms of oriented gradients (dphog). IEEE Access 7, 20894–20919.
Lee, G., Mallipeddi, R., Jang, G.-J., Lee, M., 2015. A genetic algorithm-based moving object detection for real-time traffic surveillance. IEEE Signal Process. Lett. 22, 1619–1622.
Liu, L., Lei, X., Chen, B., Shu, L., 2019. Human action recognition based on inertial sensors and complexity classification. J. Inform. Technol. Res. (JITR) 12, 18–35.
Luo, A., An, F., Zhang, X., Mattausch, H.J., 2019. A hardware-efficient recognition accelerator using haar-like feature and svm classifier. IEEE Access 7, 14472–14487.
Mahalingam, T., Subramoniam, M., 2018. A robust single and multiple moving object detection, tracking and classification. Appl. Comput. Inform.
Mohamed, A.-A.A., Hassan, S., Hemeida, A., Alkhalaf, S., Mahmoud, M., Eldin, A.M.B., 2019. Parasitism–predation algorithm (ppa): A novel approach for feature selection. Ain Shams Eng. J.
Muchtar, K., Rahman, F., Munggaran, M.R., Dwiyantoro, A.P.J., Dharmadi, R., Nugraha, I., 2019. A unified smart surveillance system incorporating adaptive foreground extraction and deep learning-based classification. 2019 International Conference on Artificial Intelligence in Information and Communication (ICAIIC). IEEE, pp. 302–305.
Patil, P., Nandyal, S., 2013. Vehicle detection and traffic assessment using images. Adv. Electron. Electric Eng. 3, 987–1000.
Saeed, A., Khan, M.J., Asghar, M.A., et al., 2019. Person detection by low-rank sparse aggregate channel features. In: Proceedings of the 7th International Conference on Communications and Broadband Networking. ACM, pp. 58–62.
Savvides, M., Lin, A.P., Venugopalan, S., Thanikkal, A., Singh, K., Adler, G., Neblett, K., 2019. Robust motion filtering for real-time video surveillance. US Patent App. 16/104,668..
Schweizer, B., 1983. B. schweizer and a. sklar, probabilistic metric spaces..
Schweizer, B., Sklar, A., et al., 1960. Statistical metric spaces. Pacific J. Math. 10, 313–334.
Sehairi, K., Chouireb, F., Meunier, J., 2018. Elderly fall detection system based on multiple shape features and motion analysis. In: 2018 International Conference on Intelligent Systems and Computer Vision (ISCV). IEEE, pp. 1–8.
Shi, L., Wan, Y., Gao, X., Wang, M., 2018. Feature selection for object-based classification of high-resolution remote sensing images based on the combination of a genetic algorithm and tabu search. Comput. Intell. Neurosci..
Soulami, K.B., Ghribi, E., Saidi, M.N., Tamtaoui, A., Kaabouch, N., 2019. Breast cancer: Segmentation of mammograms using invasive weed optimization and susan algorithms. In: 2019 IEEE International Conference on Electro Information Technology (EIT). IEEE, pp. 1–7.
Soulami, K.B., Saidi, M.N., Honnit, B., Anibou, C., Tamtaoui, A., 2018. Detection of breast abnormalities in digital mammograms using the electromagnetism-like algorithm. Multimedia Tools and Applications, (pp. 1–29)..
Soulami, K.B., Saidi, M.N., Tamtaoui, A., 2016. A cad system for the detection of abnormalities in the mammograms using the metaheuristic algorithm particle swarm optimization (pso). In: International Symposium on Ubiquitous Networking. Springer, pp. 505–517.
Soulami, K.B., Saidi, M.N., Tamtaoui, A., 2017. a cad system for the detection and classification of abnormalities in dense mammograms using electromagnetism-like optimization algorithm. In: 2017 International Conference on Advanced Technologies for Signal and Image Processing (ATSIP). IEEE, pp. 1–8.
Sun, J., Shao, J., He, C., 2019. Abnormal event detection for video surveillance using deep one-class learning. Multimedia Tools Appl. 78, 3633–3647.
UCF-Crime dataset (2018). UCF-Crime dataset. https://webpages.uncc.edu/cchen62/dataset.html..
Vijayan, M., Ramasundaram, M., 2019. A fast dgpso-motion saliency map based moving object detection. Multimedia Tools Appl. 78, 7055–7075.
Wang, Y., Ban, X., Wang, H., Wu, D., Wang, H., Yang, S., Liu, S., Lai, J., 2019. Detection and classification of moving vehicle from video using multiple spatio-temporal features. IEEE Access 7, 80287–80299.
Wei, Y., Tian, Q., Guo, J., Huang, W., Cao, J., 2019. Multi-vehicle detection algorithm through combining harr and hog features. Math. Computers Simul. 155, 130–145.
Xu, H., Li, B., Ramanishka, V., Sigal, L., Saenko, K., 2019. Joint event detection and description in continuous video streams. 2019 IEEE Winter Conference on Applications of Computer Vision (WACV). IEEE, pp. 396–405.
Zhang, Z., Tao, D., 2019. Slow feature analysis for human action recognition. arXiv preprint arXiv:1907.06670..
Zhao, J., Chen, Y., Zhuang, X., Xu, Y., 2014. Posterior probability based multi-classifier fusion in pedestrian detection. In: Genetic and Evolutionary Computing. Springer, pp. 323–329.
Zhao, J., Xu, H., Liu, H., Wu, J., Zheng, Y., Wu, D., 2019. Detection and tracking of pedestrians and vehicles using roadside lidar sensors. Transp. Res. Part C: Emerging Technol. 100, 68–87.

Please cite this article as: B. Honnit, K. B. Soulami, M. N. Saidi et al., Moving objects multi-classification based on information fusion, Journal of King Saud University – Computer and Information Sciences, https://doi.org/10.1016/j.jksuci.2020.05.003